

The structure of the Guanine Nucleotide Exchange Factor Rlf in complex with the small G-protein Ral identifies conformational intermediates of the exchange reaction and the basis for the selectivity



Milica Popovic^a, Arie Schouten^b, Marije Rensen-de Leeuw^a, Holger Rehmann^{a,*}

^a Department of Molecular Cancer Research, Centre of Biomedical Genetics and Cancer Genomics Centre, University Medical Center Utrecht, Utrecht, The Netherlands

^b Department of Crystal and Structural Chemistry, Bijvoet Center for Biomolecular Research, Utrecht University, The Netherlands

ARTICLE INFO

Article history:

Received 10 September 2015

Received in revised form 4 December 2015

Accepted 11 December 2015

Available online 11 December 2015

Keywords:

Ras-family of G-proteins

Induced fit

CDC25-homology domain

Guanine nucleotide exchange reaction

ABSTRACT

CDC25 homology domain (CDC25-HD) containing Guanine Nucleotide Exchange Factors (GEFs) initiate signalling by small G-proteins of the Ras-family. Each GEF acts on a small subset of the G-proteins only, thus providing signalling selectivity. Rlf is a GEF with selectivity for the G-proteins RalA and RalB. Here the crystal structure of Rlf in complex with Ral is determined. The Rlf-Ral complex crystallised into two different crystal forms, which represent different steps of the exchange reaction. Thereby general insight in the CDC25-HD catalysed nucleotide exchange is obtained. In addition, the basis for the selectivity of the interaction is investigated. The exchange activity is monitored by the use of recombinant proteins. Selectivity determinants in the binding interface are identified and confirmed by a mutational study.

© 2015 Elsevier Inc. All rights reserved.

1. Introduction

Small G-proteins are well recognised as molecular switches, which cycle between a GDP and a GTP bound state. Only the GTP bound state is able to interact with effector proteins to transmit the signal. Transition to the GDP bound state occurs via hydrolysis of the bound GTP by the intrinsic GTPase activity of the G-protein. This reaction is accelerated by GTPase activating proteins (GAPs). Guanine Nucleotide Exchange Factors (GEFs) catalyse the release of G-protein bound nucleotides and thereby allow rebinding of a new nucleotide. As the cellular concentration of GTP is higher than of GDP, the interaction of the GEF with the G-protein will predominantly result in GTP loading. The catalytic mechanism of the GEF reaction is based on a partial overlap of the binding interface for the nucleotide and for the GEF in the G-protein. In course of the exchange reaction, the GEF approaches the nucleotide bound G-protein such that a ternary complex is formed. In this complex the GEF is initially only loosely bound, but upon establishing its full binding interface with the G-protein the nucleotide is partially competed out of its binding site. Once loosely bound the nucleotide dissociates and a tight complex of GEF and G-protein is established.

* Corresponding author at: Molecular Cancer Research and Cancer Genomics Netherlands, Center for Molecular Medicine, UMC Utrecht, Universiteitsweg 100, 3584 CG Utrecht, The Netherlands.

E-mail address: h.rehmann@umcutrecht.nl (H. Rehmann).

By reversing these steps a nucleotide can approach the complex of GEF and G-protein, such that a ternary complex is formed and compete out the GEF. Structural information is available on the stable binary complexes (Bos et al., 2007; Vetter and Wittinghofer, 2001) but little information is available of the intermediate conformational states during the transition between the stable binary complexes.

The Ras family of small G-proteins is constituted of 36 members and sub-grouped into to “the Ras-proteins” (H-Ras, K-Ras, N-Ras, M-Ras and R-Ras), “the Ral-proteins” (RalA and RalB), “the Rap-proteins” (Rap1A, Rap1B, Rap2A, Rap2B and Rap2C) and “the rest” (the remaining 24 members). “The Ras-proteins”, are established oncogenes and frequently found mutated in tumours (Karnoub and Weinberg, 2008). The Ral-GEFs Rgl1, Rgl2/Rlf, Rgl3 and RalGDS connect Ras signalling to “the Ral-proteins”. These GEFs contain a Ras Association (RA) domain at their C-terminus which binds specifically to the GTP bound form of Ras. This allows Ras-GTP to recruit the RalGEFs to membrane compartments where Ral is localised as well. “The Ral-proteins” are involved in the control of exocytosis (Moskalenko et al., 2002), endocytosis (Jullien-Flores et al., 2000), gene regulation (de Ruiter et al., 2000) and cellular transformation (Urano et al., 1996; White et al., 1996). They are in part responsible for the transforming phenotype of oncogenic Ras mutations and recently got attention in cancer therapy due to the development of Ral-targeting small molecules (Yan et al., 2014).

In addition to the RA domain at the C-terminus Ral-GEFs contain a REM domain and a CDC25-homology domain (CDC25-HD) at the N-terminus. REM domains co-occur with CDC25-HD (Quilliam et al., 2002). They mainly stabilise the fold of the CDC25-HD but the REM-domain of SOS, a Ras-GEF, is also involved in an allosteric regulation of exchange activity (Sondermann et al., 2004). The CDC25-HD mediates the guanine nucleotide exchange activity and is found in GEFs for G-proteins of the Ras-family. While GEFs for the Ras-, Rap-, and Ral-proteins are known, GEFs for “the rest” are unknown (Popovic et al., 2013b). Based on their specificity the GEFs are classified as Ras-, Rap- and Ral-GEFs. Ral-GEFs are assumed to be truly Ral-specific (Albright et al., 1993; Ferro et al., 2008; Wolthuis et al., 1997), while some Ras-/Rap-GEFs act on both Ras- and Rap-proteins and are thus crossing the subgroup border. The selectivity of Ras- and Rap-GEFs was systematically analysed and the amino acid residues in the G-proteins that determine selectivity were identified (Popovic et al., 2013b). The findings were rationalised based on the known crystal structures of CDC25-HD in complex with small G-proteins, the crystal structures of the Ras-GEF SOS1 in complex with H-Ras (Boriack-Sjodin et al., 1998) and the Rap-GEF Epac2 in complex with Rap1B (Rehmann et al., 2008). However, the selectivity of RalGEFs was not analysed and it is unclear how selectivity towards Ral-proteins is achieved. This aspect will be addressed here.

2. Materials and methods

2.1. Protein purification

Several constructs of Ral homologues were expressed as GST-fusion proteins from pGEX4T3: RalB *Homo sapiens* amino acids 1–206, 1–179 and 12–179; RalA *Saguinus oedipus* amino acids 1–206, 1–179 and 12–179; and dRal *Drosophila melanogaster* amino acids 1–201, 1–176, 10–176 and 10–201. The GST-tag was removed by thrombin cleavage as described (Rehmann, 2006). Rlf (Rgl2, *Mus musculus* amino acid 50–514) was expressed and purified as described (Popovic et al., 2013a).

2.2. Determination of GEF activity

The exchange activity is measured in a fluorescence-based assay, for which the G-protein is loaded with the fluorescent GDP analogue mGDP. The fluorescence intensity of mGDP is approximately twice as high if bound to a G-protein as of free mGDP in solution. In the presence of an excess of unlabelled nucleotide the exchange reaction can be monitored as a decay of the fluorescence signal. The decay is single exponential and the corresponding rate constant k_{obs} is a measure of exchange activity (Rehmann, 2006). Experiments were performed as described (Popovic et al., 2013b). The concentration of the G-protein was

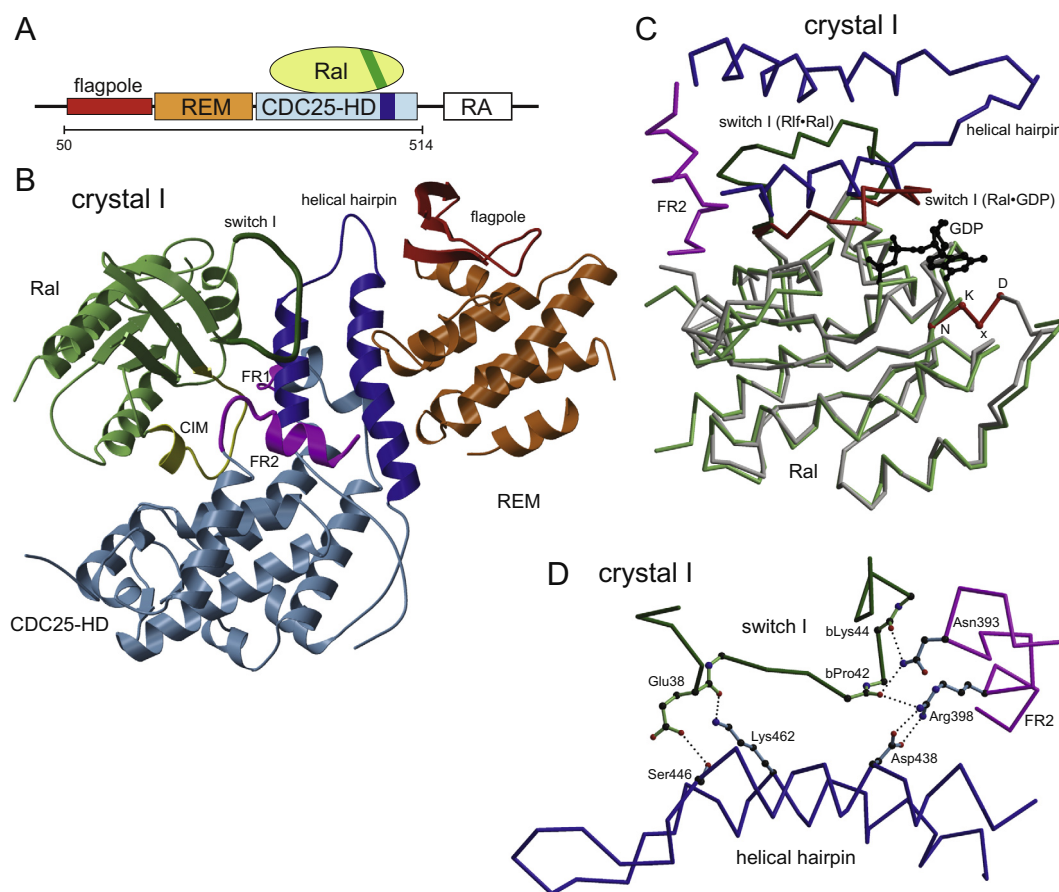


Fig. 1. Crystal structure of Rlf in complex with dRal. (A) Domain organisation of Rlf. The construct used for crystallisation is indicated. The colour code is used throughout the figures. REM, Ras Exchange Motif; CDC25-HD, CDC25-homology domain; RA, Ras-Association. (B) Ribbon diagram of Rlf⁵⁰⁻⁵¹⁴ in complex with dRal based on the model of crystal I. The helical hairpin is highlighted in dark blue and switch I in dark green. The flexible region 1 (FR1), which is unstructured in the Ral-free Rlf and the flexible region 2 (FR2), which is flexible in the Ral-free Rlf and in crystal II, are shown in magenta. CIM, core interaction motif (yellow). (C) Superposition of GDP bound Ral (Protein Data bank entry 1U90) shown in grey upon the nucleotide free Ral from the Rlf-Ral complex of crystal I. GDP is in ball-and-stick representation in black. Switch I and the NKxD motif of Ral-GDP are highlighted in red. (D) Detailed view of the interactions between the helical hairpin and switch I.

Table 1
Data collection and refinement statistic.

Protein ^a PDB entry	Crystal I (5CM8)	Crystal II (5CM9)
<i>Data collection</i>		
Space group	C121	C121
Cell dimensions (Å)	<i>a</i> = 111.1 <i>b</i> = 98.5 <i>c</i> = 71.3	<i>a</i> = 169.9 <i>b</i> = 99.8 <i>c</i> = 111.5
Cell angles (°)	α = 90 β = 91.6 γ = 90	α = 90 β = 127.0 γ = 90
Unit cell volume (Å ³)	780,164	1,509,983
Wavelength (Å)	0.95372	0.97488
Resolution range (Å) ^b	50–2.6 (2.7–2.6)	50–2.6 (2.7–2.6)
Number of reflections	71,227	115,791
Number unique reflections	23,162	40,751
Completeness (%) ^b	97.7 (99.6)	88.5 (56.8)
Redundancy ^b	3.1 (3.2)	2.8 (1.8)
<i>I</i> / σ ^b	15.8 (3.2)	12.7 (2.7)
<i>R</i> _{meas} (%) ^b	5.6 (39.3)	6.9 (33.9)
<i>Refinement</i>		
<i>R</i> _{cryst} (%)	25.9	27.3
<i>R</i> _{free} (%) ^c	32.2	32.0
Number of atoms		
Protein	4589	8583
Water	45	36
Average <i>B</i> factor (Å ²)		
Protein	65.1	58.4
Rlf	55.6	50.8
Ral	89.0	78.5
Water	52.1	49.4
rmsd from ideal values:		
Bond lengths (Å)	0.007	0.007
Bond angles (°)	1.037	1.038

^a Data collection statistic for each complex correspond to a data set derived from a single crystal.

^b Values in parenthesis correspond to highest resolution shell.

^c The free-*R* factor was calculated with 5% of the data omitted from structure refinement.

^d Alternative cell choice for crystal II.

200 nM in all experiments, the concentration of the GEF was 150 nM or 1500 nM.

2.3. Crystallography

Rlf^{50–514} in complex with different Ral constructs was subjected to crystallisation trials. Only Rlf^{50–514}.dRal^{1–201} resulted in crystals. The initial hit was optimised and final crystals were grown at 289 K in sitting drops using a reservoir solution containing 15% PEG 3350, 200 mM ammonium acetate and 100 mM Bis-Tris propane, pH 7.45. Data sets from two crystals obtained from the same condition were collected at 100 K at beamline ID23-1 of ESRF and processed with XDS (Kabsch, 1993). Crystal I was cryo-protected in a solution containing the mother liquor supplemented with 40% PEG 200 and crystal II containing the mother liquor supplemented with 60% trehalose. Molecular replacement was carried out in MOLREP (Vagin and Teplyakov, 2000) using Rlf^{50–514} (PDB entry 4JGW) as poly-alanine search model. The program O (Jones et al., 1991) was used to build the model into $2F_o - F_c$ and $F_o - F_c$ maps and refinement was carried out with REFMAC (Murshudov et al., 1997). The Ramachandran plot of crystal I depicts 92.4% of main chain torsion angles in the most favoured and 7.6% in additional allowed regions with 0 residues in generously allowed or disallowed regions. The Ramachandran plot of crystal II depicts 82.8% of main chain torsion angles in the most favoured and 7.2% in additional allowed regions with 0 residues in generously allowed or disallowed regions.

Figures were generated using the programs Molscript (Kraulis, 1991), Bragi (Schomburg and Reichelt, 1988) and Raster3D (Merritt and Murphy, 1994).

2.4. Co-ordinates

Co-ordinates and structure factors have been deposited in the Protein Data Base with the accession codes 5CM8 (crystal I) and 5CM9 (crystal II).

3. Results and discussion

3.1. Crystal structure of the Rlf-dRal complex

Diffraction crystals were obtained from a complex of a truncated construct of Rlf containing residues 50–514 (referred to as Rlf here after) and the homologue of Ral from *Drosophila* (Fig. 1A, B and Table 1). The Rlf construct contains the REM domain and the CDC25-HD but lacks the RA domain. It displays similar catalytic activity as full length Rlf (Popovic et al., 2013a). Structures obtained from two crystals belonging to two different forms were solved and refined. The data sets for form I and II were collected from a crystal frozen with PEG200 and trehalose as cryo-protectant, respectively. However, both forms were observed with both cryo-protectants (Suppl. Table 1). The overall topology of the Rlf-dRal complex is similar in both crystals and general features of the structure will be discussed first based on crystal I. The REM domain and the CDC25-HD are arranged as in the structure of the Ral-free Rlf (Popovic et al., 2013a). The REM domain shields some hydrophobic side chains of residues localised in the helical hairpin of the CDC25-HD. In addition, it positions the so-called flagpole (Fig. 1B). The flagpole is a long three stranded β -sheet that protrudes outwards of the otherwise rather compact structure. It contains at its tip a proline-rich motif for the interactions with SH3 domains (Popovic et al., 2013a). Ral is nucleotide free. The interaction of Ral is limited to the CDC25-HD and no contacts with the REM domain or the flagpole are observed (Fig. 1B).

The overall binding mode of Ral and Rlf is similar to the interaction of Ras with the CDC25-HD of SOS1 (Boriack-Sjodin et al., 1998) and of Rap1B with the CDC25-HD of Epac2 (Rehmann et al., 2008). The binding interface in the CDC25-HD is arranged like a chair with the core of the domain as the seating and the helical hairpin as the backrest (Fig. 1B). The interactions with the domain core are mainly mediated by residues 64–79 of Ral, which will be referred to as the core interaction motif. This region corresponds to residues 56–70 of H-Ras and is known to contain critical determinants for the selectivity for the interaction between GEF and G-protein (Popovic et al., 2013b). The helical hairpin is inserted into the nucleotide binding site and interacts with the switch I region (Fig. 1C and D). In consequence switch I is bent away from the nucleotide binding site. This results in an open nucleotide binding site incompatible with nucleotide binding.

The remaining parts of the nucleotide-free Ral are similar to structures of *S. oedipus* RalA bound to GDP or the GTP analogue GppNHP. Nevertheless two additional regions are notable. First, the loop containing the NKxD motif is unstructured in the nucleotide free Ral of the Rlf-dRal complex. The NKxD motif is highly conserved in small G-proteins and mediates interactions with the base of the nucleotide. Second, parts of the core interaction motif are unstructured in several nucleotide bound structures (PDB 1u8z, Ral-GDP, 2 molecules per ASU, residues 69–71 unstructured; PDB 1u90, Ral-GDP, 2 molecules per ASU, region defined; PDB 1u8y, 2 molecules per ASU, molecule A: residues 69–79 unstructured and molecule B: region defined (dRal numbering)) (Nicely et al., 2004). It thus seems that the core interaction motif is characterised by high intrinsic flexibility. Likewise, residues 273–282 of Ral-free Rlf, which are involved in interactions with the core interaction motif, are flexible and are referred to here as Flexible Region 1.

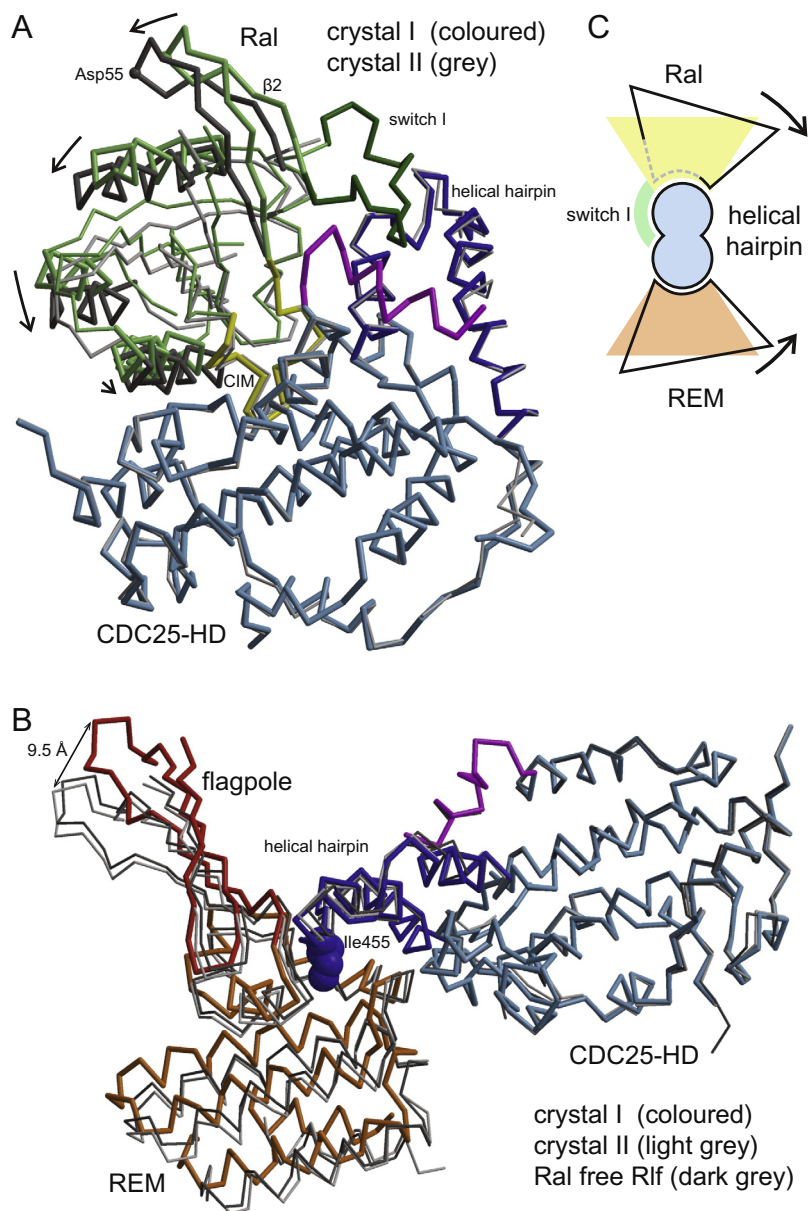


Fig. 2. Orientation of Ral and the REM domain. (A) The CDC25-HDs of the models of crystal I (shown in colour) and II (shown in grey) were superimposed upon each other. For clarity of presentation several structural elements of Ral are represented with thick traces and light and dark grey is altered. The direction of the rotation with the core interaction motif (yellow) as pivot axis is indicated by arrows. The position of Asp55 in Ral is indicated. $\beta 2$, second β -strand of Ral. (B) The CDC25-HDs of the model from crystal II (shown in light grey) and of Ral-free Rlf (shown in dark grey; Protein Data bank entry 4JGW (Popovic et al., 2013a)) were superimposed upon the model from crystal I (shown in colour). The side chain of Ile455^{Rlf}, a hydrophobic residue of the helical hairpin that is shielded by the REM domain, is represented as space filling (CPK model). (C) Schematic representation of the relative orientation of Ral and the REM domain in relation to the helical hairpin. Crystal I represented by colour, crystal II represented by outline. Switch I (dark green) is ordered only in crystal I where it “embraces” the helical hairpin.

3.2. Conformational steps in course of the exchange reaction

The orientations of Ral and the REM domain relative to the CDC25-HD slightly differ in both crystals (Fig. 2). The REM domain is slightly rotated with the helical hairpin as the pivot axis. The rotation has little impact on the residues of the REM domain in direct proximity to the helical hairpin. In both situations the REM domain fulfils its function to shield hydrophobic residues of the helical hairpin. The tip of the flagpole, which is most distal to the pivot axis, is moved by 9.5 Å. The orientation of the REM domain in crystal II corresponds to the orientation found in the Ral-free Rlf (Fig. 2B).

Similarly, Ral is rotated by approximately 1° (Fig. 2A). The core interaction motif functions as the pivot axis. The interactions

between the core interaction motif and the CDC25-HD are therefore only minimally affected. On the other hand, the distance of $\beta 2$ to the helical hairpin is increased in crystal II. $\beta 2$ is N-terminally preceded by switch I, therefore switch I has to follow the movement of $\beta 2$. In crystal II switch I is unstructured as are residues 389–402 of the CDC25-HD. In crystal I these residues constitute a loop and a helix and interact with switch I (Fig. 1D). Likewise residues 389–396 of the Ral-free Rlf are unstructured (Fig. 1B). This region of Rlf is therefore referred to as Flexible Region 2. The orientation of the REM domain and of Ral are likely independent of each other. No direct contacts are observed between the REM domain and Ral.

The packing of both crystals is almost identical, even though crystal I and crystal II contain one and two complexes per

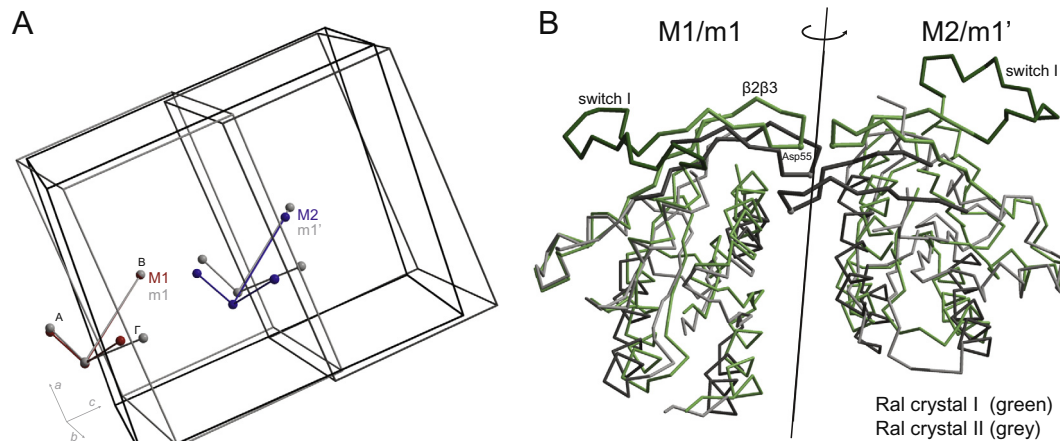


Fig. 3. Packing of crystal I and II. (A) The asymmetric unit of crystal II, which is constituted by the complexes M1 (red) and M2 (blue), is shown together with the *I*121 cell in black. The CDC25-HD domain of the complex from crystal I (m1, grey) was superimposed onto M1. The deviation of the Γ -arm reflects the different orientations of the flagpoles. m1' is a symmetry related complex of m1. Note, m1' is more distant to M1 than M2. In relation to m1 the unit cell of crystal I (C121) is shown in light grey. The crystal I unit cell after superimposing crystal I onto M2 is shown in dark grey. The region around Asp55 in the loop between $\beta 2$ and $\beta 3$ forms a crystal contact. (B) Two Ral molecules belonging to the lattice of crystal II are shown in grey. The strands $\beta 2$ and $\beta 3$ are shown in dark grey. The region around Asp55 in the loop between $\beta 2$ and $\beta 3$ forms a crystal contact. The green Ral molecules belong to the lattice of crystal I. Switch I in depicted in dark green. The positions were obtained as follows: The left green Ral molecule belongs to a CDC25-HD, which was superimposed upon the CDC25-HD of the left grey Ral molecule. The right green Ral is a symmetry related molecule of the left green Ral. The two fold rotation axis by which these two molecules are related based on the crystal I lattice is indicated.

asymmetric unit. Thus the same regions of the proteins form similar contacts. The two complexes in the asymmetric unit of crystal II are related by a translation that is slightly off from the crystallographic *c*-axis. In crystal I the equivalent to the second complex is positioned slightly more distant and slightly more “up” and thereby becomes a crystallographic symmetry mate related by a twofold rotation axis (Fig. 3A and Suppl. Fig. 1).

The packing is directly related to the relative orientation of Ral and the REM domain towards the CDC25-HD. In both crystals the $\beta 2\beta 3$ -loops of two Ral molecules are in contact with each other, albeit in a different manner. In crystal I the tips of the loop face each other and a twofold axis goes through the contact interface (Fig. 3B). In crystal II Ral is partially rotated out of the binding site at the CDC25-HD. In crystal I this rotation would move the $\beta 2\beta 3$ -loops towards each other and cause a clash. The rotation would also place the $\beta 2\beta 3$ -loops “on” the twofold axis. To allow the rotation of Ral out of the binding site one complex is shifted slightly “downwards” in crystal II. This enables the two $\beta 2\beta 3$ -loops to interlace in a zipper like fashion (Fig. 3B). The rotation symmetry between the complexes is lost, but the zipper-like arrangement allows the complexes to move closer to each other.

The interaction between Rlf and Ral in crystal II appears “looser” than in crystal I. Crystal II seems to represent a step in course of establishing or releasing the full interaction. Based on the differences between crystal I and II the putative sequence of events will be discussed here as the release process. In the fully bound state switch I interacts with the helical hairpin and with the flexible region 2 of Rlf. Switch I “embraces” the helical hairpin and is stabilised in the bent open conformation of the nucleotide free state of Ral. As the first step of Ral release the interaction with switch I is disrupted. The release of the “embrace” is precondition to move Ral and Rlf apart. Ral then rotates slightly away from the helical hairpin, which prevents switch I from rebinding. Switch I and flexible region 2 in Rlf are now unstructured. This state is seen in crystal II. In the next step the interaction between the core interaction motif and Rlf gets disrupted accompanied by the initiation of nucleotide rebinding to Ral. The interaction of the core interaction motif is already weakened by the rotation (see below). If released, the core interaction motif and the flexible region 1 of Rlf are less constrained and become unstructured.

3.3. Ral related selectivity

The activity of Rlf is determined at a fixed concentration of GEF and G-protein following a standardised approach that allows the comparison of different GEFs and G-proteins (Popovic et al., 2013b). Rlf-induced nucleotide exchange rates (k_{obs}) are similar for dRal and the mammalian homologues RalA and RalB, suggesting that structural information obtained with dRal is of common relevance (Fig. 4).

Typically k_{obs} can be monitored conveniently if the GEF is used at a concentration of 150 nM. However, some GEFs like SOS1 display only weak exchange activity at this concentration towards their well-established target G-proteins and therefore in these cases a concentration of 1500 nM is used (Popovic et al., 2013b). At 150 nM the exchange activity of Rlf towards Ral-proteins is weaker than the activity of RapGEFs typically observed with Rap-proteins (Fig. 4). Therefore, Rlf activity is monitored at both concentrations.

Next to Rlf the exchange activity of the Ras- and Rap-GEFs SOS1, RasGRP1, RasGRP2, RasGRP3, Epac1, Epac2, C3G, PDZ-GEF1 and PDZ-GEF2 towards RalA and RalB was monitored. None of the Ras- and Rap-GEFs act on RalA or RalB (Fig. 4B). Under the same reaction conditions the Ras- and Rap-GEFs show pronounced activity towards either H-Ras or Rap1B or to H-Ras and Rap1B. H-Ras and Rap1B were chosen as representatives of the Ras- and the Rap-proteins, as structural information of SOS1-H-Ras (Boriack-Sjodin et al., 1998) and Epac2-Rap1B (Rehmann et al., 2008) is available and as H-Ras and Rap1B were subjected to an extensive mutagenesis study to study the basis of GEF selectivity (Popovic et al., 2013b). In contrast, Rlf does not act on H-Ras or Rap1B under conditions where it acts readily with RalA and RalB (Fig. 4B). This confirms the strict border between the Ral-proteins and their GEFs on one side and the Ras- and Rap-proteins and their GEFs on the other side.

3.4. Structural basis for the selectivity of the GEF reaction

In primary structure Ral is most similar to the Ras-proteins. Within the core interaction motif diverging amino acids are found at four positions: Glu63^{Ras}/Asp71^{Ral}, Ser65^{Ras}/Ala73^{Ral}, Met67^{Ras}/

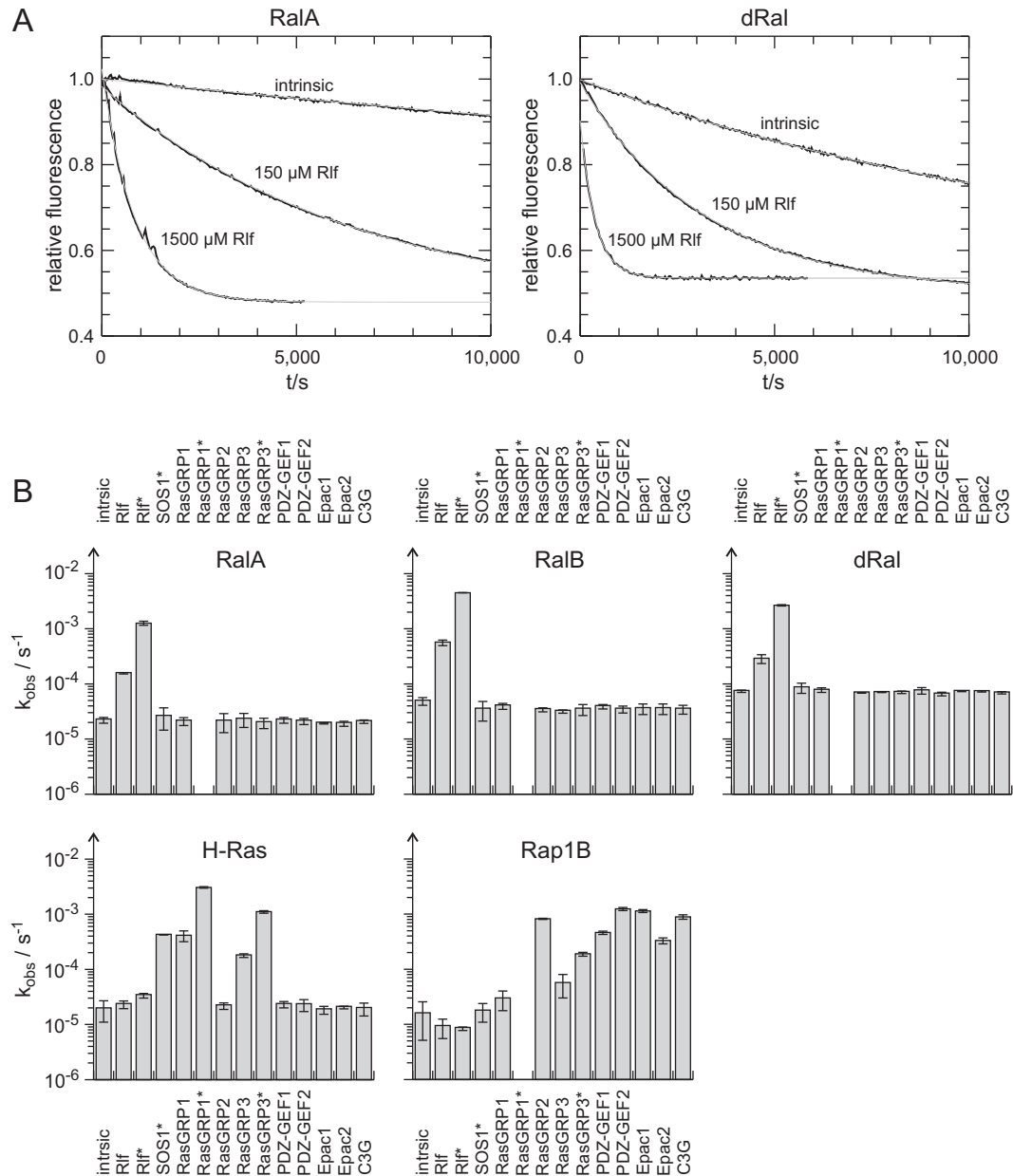


Fig. 4. Selectivity of CDC25-HD domain containing GEFs. (A) Rlf-catalysed nucleotide exchange reaction of RalA and dRal. Nucleotide exchange is observed as decay in the fluorescence signal. The data are fitted as single exponential decay with off-set (grey lines) to obtain the rate constant k_{obs} . (B) The selectivity of the indicated GEFs for RalA, RalB, dRal, H-Ras and Rap1B were determined in triplicate and the obtained rate constants (k_{obs}) are presented as bar diagrams on a logarithmic scale. *GEF is added at 1500 nM instead of 150 nM. If added at 1500 nM RasGRP1 precipitates out of solution after approximately 3–4 h. This makes it impossible to determine slow exchange rates in the presents of high concentrations of RasGRP1.

Ile75^{Ral} and Gln70^{Ras}/Asn78^{Ral} (Suppl. Fig. 2A). To analyse the importance of these residues for the interaction of Ral with Rlf, the residues were mutated to the corresponding residue in Ras either individually or in combination (Fig. 5A). Rlf does not catalyse nucleotide exchange of Ral^{D71E,A73S,I75M,N78Q}. The effect of the individual mutations is more differentiated. Nucleotide exchange is slightly reduced for Ral^{A73S} and strongly reduced for Ral^{D71E} and Ral^{I75M}. Interestingly, a slight enhancement of Rlf mediated nucleotide exchange is observed for Ral^{N78Q} (Fig. 5A). However, none of these Ral mutants gains the ability to interact with the Ras-GEFs SOS1, RasGRP1 or RasGRP3, even not if these GEFs are used at a concentrations of 1500 nM. Also the introduction of additional mutations outside of the core interaction region does not result in the ability to interact with Ras-GEFs. The interaction of

Ras-GEFs with the mutated Ral would require that the mutated residues are “presented” to the GEF as by H-Ras. In addition, the mutated residues have to accommodate to constrain originating from the remaining parts of the protein. An approach to identify such constraints failed as upon accumulation of mutations the protein became unstable (Suppl. Fig. 3).

If the corresponding mutations are introduced in Ras, the ability to interact with Rlf is stepwise gained (Fig. 5B). Rlf induces nucleotide exchange of Ras^{E63D,M67I} and even stronger of Ras^{E63D,S65A,M67I}. No additional activity is gained for Ras^{E63D,S65A,M67I,Q70N}. The activity level of Rlf for mutated Ras is comparable to that of RasGEFs for wild type Ras. The activity of SOS1 towards Ras is gradually lost with increasing number of mutations. The effect of the mutations on RasGRP1 and RasGRP3 catalysed exchange is more subtle, for

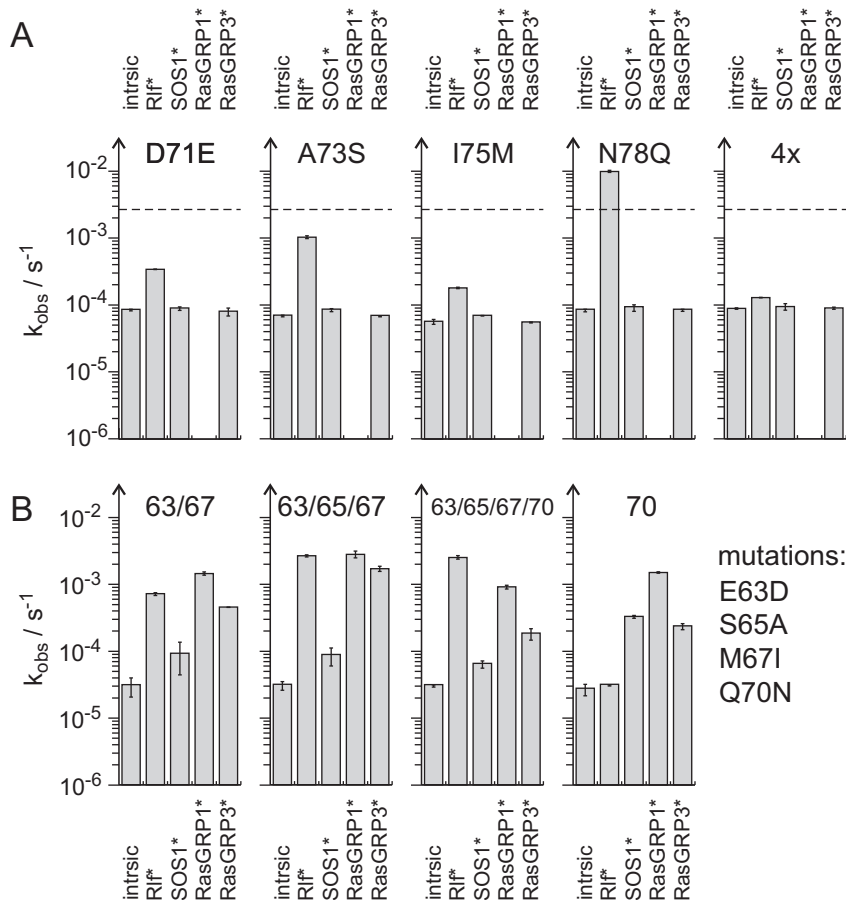


Fig. 5. Mutational study of Ral and H-Ras. GEF activity of Rlf and Ras-GEFs was determined as in Fig. 4. dRal was mutated to the corresponding amino acid residues in H-Ras and H-Ras was mutated to the corresponding amino acid residues in dRal. (A) Activity for mutated dRal proteins. The dashed line indicated the activity of Rlf to dRal wild type. (B) Activity for mutated H-Ras proteins.

example hardly any impairment is seen for Ras^{E63D,S65A,M67I}. This likely reflects the dual selectivity of the RasGRP family towards Ras and Rap. While RasGRP1 acts as RasGEF and RasGRP2 as RapGEF, RasGRP3 acts as Ras- and RapGEF. For example, Gln70^{Ras} corresponds to Leu70^{Rap}. This difference is used by “normal” RasGEFs and RapGEFs to discriminate between Ras and Rap. Due to their dual specificity RasGRPs can adapt to a wider sequence diversity.

Asp71^{Ral} and Ile75^{Ral} are core requirements for efficient catalysis by the RalGEF Rlf. Within the Ras family these residues are a unique feature of Ral proteins (Suppl. Fig. 2B). An Isoleucine residue at position 75^{Ral} is exclusively found in the Ral proteins. Except in Ral proteins, only in NKIRas2 and Rrad an Aspartate is found at position 71^{Ral}, but in these proteins the remaining core interaction motif is not conserved. Interestingly, also an Asparagine at position 78^{Ral} is an exclusive feature of Ral proteins, even though Rlf catalysed exchange activity is enhanced for Ral^{N78Q}. In this sense the interactions of Ral with Rlf are not the cause of evolutionary pressure towards conservation of Asn78^{Ral}. On the other hand Asn78^{Ral} is also involved in the interaction with the Ral effectors Rlip (PDB data base entry 2KWI) (Fenwick et al., 2010) and exocyst complex component 8 (PDB data base entries 1ZC3 and 1ZC4) (Jin et al., 2005).

The effect of the Ras and Ral mutants on the Rlf and SOS1 catalysed exchange activity is supported by the structural features of the binding interface. Asp71^{Ral} and Asp70^{Ral} interact with Arg275^{Rlf} (Fig. 6A). This interaction is found in crystal I and in both complexes of crystal II. Seeming differences in the conformation of the side chain of Arg275^{Rlf} are found. All molecules were refined

independently and the differences are likely reflecting possible alternative conformations within the resolution limit of the crystals (Fig. 6A). A similar interaction with the longer side chain of Glu63^{Ras} is impossible, which explains the strong reduction of the exchange activity of Rlf for Ral^{D71E}.

The backbone nitrogen atom of Ala73^{Ral} forms a hydrogen bond with Asn295^{Rlf} (Fig. 6B). Asn295^{Rlf} is in addition hydrogen-bonded to the backbone oxygen of Asp71^{Ral}. Ala73^{Ral} corresponds to Ser65^{Ras}. In the structure of SOS1-Ras the backbone is kinked differently and the backbone nitrogen of Ser65^{Ras} is at a different position. The difference in kinking is not necessarily a consequence of the substitution of alanine for serine as the positions of the CA atoms of the residues in the adjacent region differ. In agreement with this considerations the exchange activity of Rlf for Ral^{A73S} is only minimally affected (Fig. 5).

Ile75^{Ral} is inserted in a hydrophobic pocket formed by the CDC25-HD (Fig. 6C). This pocket would not be able to accommodate the sterically more demanding methionine. This explains the crucial importance of Ile75^{Ral} for Rlf-mediated exchange activity (Fig. 5). A wider hydrophobic pocket is formed in SOS1 by smaller amino acids (Fig. 6C). The majority of the surrounding of Ile75^{Ral} is similar in crystal I and II. However, Tyr394^{Rlf} is part of flexible region 2 and thus “absent” from the hydrophobic pocket in crystal form II. In consequence, the phenyl ring of Tyr79^{Ral} in direct proximity to Ile75^{Ral} is rotated differently (Fig. 6D).

Asn78^{Ral} directly interacts with Glu398^{Rlf}, which is part of flexible region 2 and with Gln359^{Rlf}, which is part of the core CDC25-HD (Fig. 6E). In crystal II χ_1 of Asn78^{Ral} is turned by about

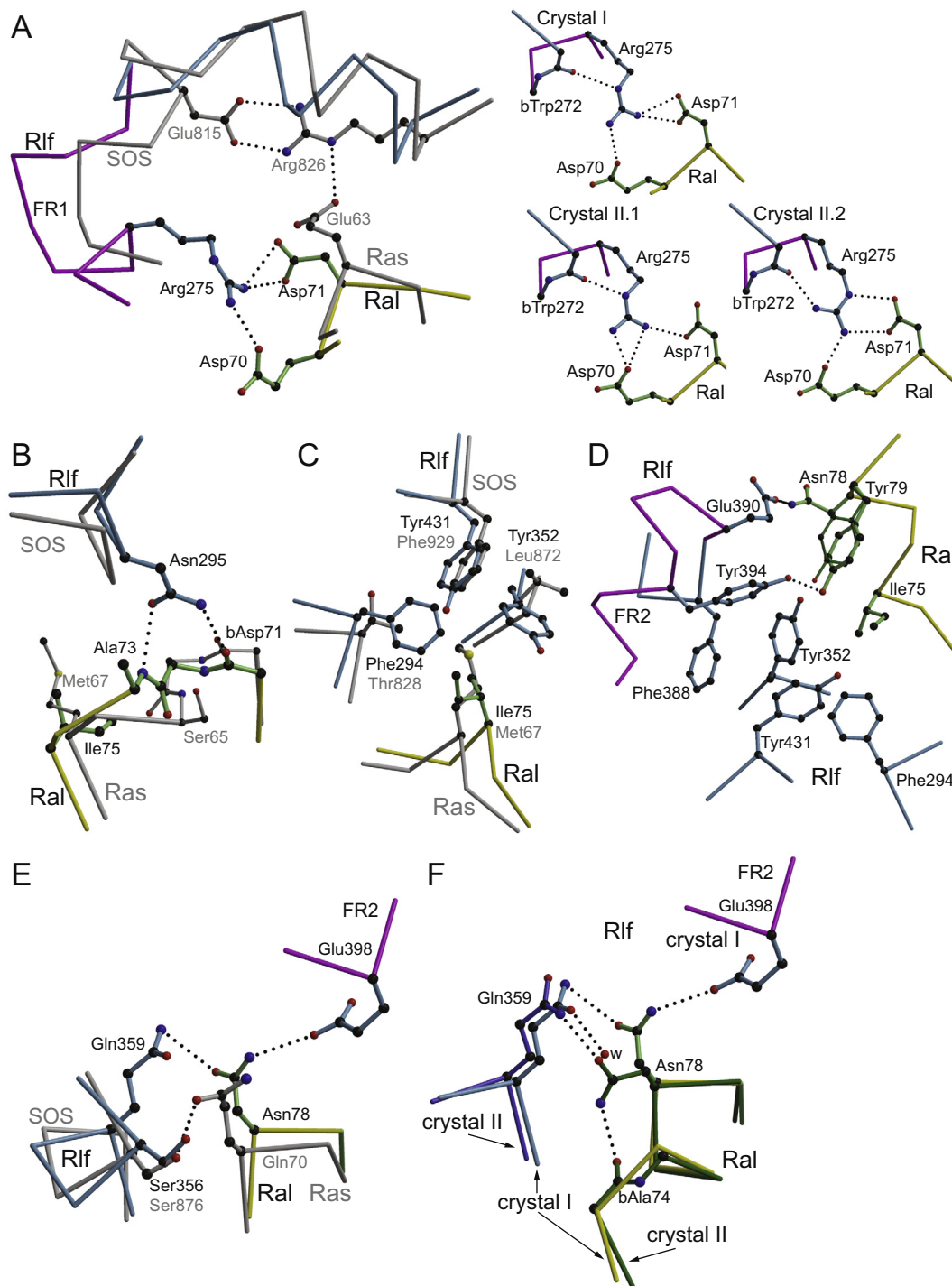


Fig. 6. Comparison of the GEF-G-protein interaction in the Rlf-Ral and the SOS1-H-Ras complex. The G-proteins of the Rlf-Ral complex and the SOS1-H-Ras complex (PDB database entry 1BKD (Boriack-Sjodin et al., 1998)) were superimposed upon each other. If not indicated otherwise crystal II is shown. Rlf is shown in blue with the flexible regions (FR1 and FR2) in magenta, Ral in green with the core interaction motif in yellow and SOS and Ras in grey. Hydrogen bonds are indicated by dotted lines. Amino acid residues are labelled by the three letter code; b indicates that only the backbone is depicted. (A) Region around Asp71^{Ral} and Glu63^{Ras}. The smaller panels on the right depict the conformation of Arg275^{Rlf} in crystal I and in the two molecules of crystal II. (B) Region around Ala73^{Ral} and Ser65^{Ras}. (C) Region around Ile75^{Ral} and Met67^{Ras}. (D) Region around Ile75^{Ral} in crystal I and crystal II. From crystal II only Tyr79^{Ral} is depicted in dark green. (E) Region around Asn78^{Ral} and Gln70^{Ras}. (F) Region around Asn78^{Ral} in crystal I and II. Crystal II is presented in dark blue and dark green.

90° (Fig. 6F). An interaction with Gln359^{Rlf} is maintained and in addition a hydrogen bond with the backbone oxygen of Ala74^{Ral} is formed. Gln70^{Ras} interacts with Ser876^{SOS} in the core the CDC2-HD. This Serine is conserved in Rlf. This might explain why the catalytic activity of Rlf is higher for Ral^{N78Q} than for wild type Ral (Fig. 5).

4. Conclusions

Rlf acts exclusively as a GEF for Ral-proteins. The structural and mutational study presented here has identified amino acid residues that are critical for the selective recognition of Ral by Rlf. Asp71^{Ral} and Ile75^{Ral} are crucial for the Rlf-catalysed exchange

reaction. Mutations of these residues in Ral result in the loss of Rlf-catalysed exchange activity. Furthermore, if the corresponding residues in Ras, the G-protein of the Ras-family that has the highest sequence homology to Ral, are mutated, Rlf-mediated exchange activity is gained. Indeed, an Aspartate and Isoleucine at position 71 and 75, respectively, are only found in Ral-proteins.

The structure of the Rlf-Ral complex was solved in two different conformational states with the REM domain and Ral differently orientated relative to the CDC25-HD. The full interaction is established in crystal I, where switch I is engaged in interactions with the helical hairpin. In crystal II the interaction of switch II is lost and the interactions by the core interaction motif are partially weakened. The nucleotide-binding site is partially occupied by the CDC25-HD and thus Ral is nucleotide free in both crystal forms. Also, no density for an approaching nucleotide is seen. The weakening of the interaction between Ral and Rlf, which would occur upon transition from the conformation in crystal I to that in crystal II, is thus independent of nucleotide rebinding. The course of the GEF catalysed exchange reaction is commonly considered as transitions between the stable complexes of GEF and G-protein, and of GEF and nucleotide, respectively, with the transient complex of GEF, G-protein and nucleotide. Here we provide arguments that the GEF-G-protein complex is established in a stepwise process from a looser to a tighter bound state. Several elements of the interacting regions in Ral and in Rlf are flexible in the absence of the interaction. The binding of Ral to Rlf is an induced fit process, in which the flexibility of parts of the later interaction interface allow the two molecules to approach each other.

Acknowledgements

We thank Piet Gros for access to crystallisation robots, Martin Lutz for discussion, the European Synchrotron Radiation Facility for providing synchrotron facilities and the scientists at ESRF_ID23-1 for help with data collection. M.P. and M.R.d.L. were supported by the TI Pharma Project T3-106 to J.L. Bos, and H.R. by the Chemical Sciences of the Netherlands Organization for Scientific Research (NWO).

Appendix A. Supplementary data

Supplementary data associated with this article can be found, in the online version, at <http://dx.doi.org/10.1016/j.jsb.2015.12.006>.

References

Albright, C.F., Giddings, B.W., Liu, J., Vito, M., Weinberg, R.A., 1993. Characterization of a guanine nucleotide dissociation stimulator for a ras-related GTPase. *EMBO J.* 12, 339–347.

Boriack-Sjodin, P.A., Margarit, S.M., Bar-Sagi, D., Kuriyan, J., 1998. The structural basis of the activation of Ras by Sos. *Nature* 394, 337–343.

Bos, J.L., Rehmann, H., Wittinghofer, A., 2007. GEFs and GAPs: critical elements in the control of small G proteins. *Cell* 129, 865–877.

de Ruiter, N.D., Wolthuis, R.M., van, D.H., Burgering, B.M., Bos, J.L., 2000. Ras-dependent regulation of c-Jun phosphorylation is mediated by the Ral guanine nucleotide exchange factor-Ral pathway. *Mol. Cell. Biol.* 20, 8480–8488.

Fenwick, R.B., Campbell, L.J., Rajasekar, K., Prasannan, S., Nietlispach, D., Camonis, J., Owen, D., Mott, H.R., 2010. The RalB-RLIP76 complex reveals a novel mode of ral-effector interaction. *Structure* 18, 985–995.

Ferro, E., Magrini, D., Guazzi, P., Fischer, T.H., Pistolesi, S., Pogni, R., White, G.C., Trabalzini, L., 2008. G-protein binding features and regulation of the RalGDS family member, RGL2. *Biochem. J.* 415, 145–154.

Jin, R., Junutula, J.R., Matern, H.T., Ervin, K.E., Scheller, R.H., Brunger, A.T., 2005. Exo84 and Sec5 are competitive regulatory Sec6/8 effectors to the RalA GTPase. *EMBO J.* 24, 2064–2074.

Jones, T.A., Zou, J.Y., Cowan, S.W., Kjeldgaard, M., 1991. Improved methods for building protein models in electron-density maps and the location of errors in these models. *Acta Crystallogr. A* 47, 110–119.

Jullien-Flores, V., Mahe, Y., Mirey, G., Leprince, C., Meunier-Biscueil, B., Sorkin, A., Camonis, J.H., 2000. RLIP76, an effector of the GTPase Ral, interacts with the AP2 complex: involvement of the Ral pathway in receptor endocytosis. *J. Cell Sci.* 113 (Pt. 16), 2837–2844.

Kabsch, W., 1993. Automatic processing of rotation diffraction data from crystals of initially unknown symmetry and cell constants. *J. Appl. Crystallogr.* 26, 795–800.

Karnoub, A.E., Weinberg, R.A., 2008. Ras oncogenes: split personalities. *Nat. Rev. Mol. Cell Biol.* 9, 517–531.

Kraulis, P.J., 1991. Molscript – a program to produce both detailed and schematic plots of protein structures. *J. Appl. Crystallogr.* 24, 946–950.

Merritt, E.A., Murphy, M.E.P., 1994. Raster3D version-2.0 – a program for photorealistic molecular graphics. *Acta Crystallogr. D Biol. Crystallogr.* 50, 869–873.

Moskalenko, S., Henry, D.O., Rosse, C., Mirey, G., Camonis, J.H., White, M.A., 2002. The exocyst is a Ral effector complex. *Nat. Cell Biol.* 4, 66–72.

Murshudov, G.N., Vagin, A.A., Dodson, E.J., 1997. Refinement of macromolecular structures by the maximum-likelihood method. *Acta Crystallogr. D Biol. Crystallogr.* 53, 240–255.

Nicely, N.I., Kosak, J., de Serrano, V., Mattos, C., 2004. Crystal structures of Ral-GppNHp and Ral-GDP reveal two binding sites that are also present in Ras and Rap. *Structure* 12, 2025–2036.

Popovic, M., Jakobi, A.J., Rensen-de Leeuw, M., Rehmann, H., 2013a. The guanine nucleotide exchange factor Rlf interacts with SH3 domain-containing proteins via a binding site with a preselected conformation. *J. Struct. Biol.* 183, 312–319.

Popovic, M., Rensen-de, L.M., Rehmann, H., 2013b. Selectivity of CDC25 homology domain-containing guanine nucleotide exchange factors. *J. Mol. Biol.* 425, 2782–2794.

Quilliam, L.A., Rebhun, J.F., Castro, A.F., 2002. A growing family of guanine nucleotide exchange factors is responsible for activation of Ras-family GTPases. *Prog. Nucleic Acid Res. Mol. Biol.* 71, 391–444.

Rehmann, H., 2006. Characterization of the activation of the Rap-specific exchange factor Epac by cyclic nucleotides. *Methods Enzymol.* 407, 159–173.

Rehmann, H., Arias-Palomo, E., Hadders, M.A., Schwede, F., Llorca, O., Bos, J.L., 2008. Structure of Epac2 in complex with a cyclic AMP analogue and RAP1B. *Nature* 455, 124–127.

Schomburg, D., Reichelt, J., 1988. Bragi – a comprehensive protein modeling program system. *J. Mol. Graph.* 6, 161–165.

Sondermann, H., Soisson, S.M., Boykevich, S., Yang, S.S., Bar-Sagi, D., Kuriyan, J., 2004. Structural analysis of autoinhibition in the Ras activator Son of sevenless. *Cell* 119, 393–405.

Urano, T., Emkey, R., Feig, L.A., 1996. Ral-GTPases mediate a distinct downstream signaling pathway from Ras that facilitates cellular transformation. *EMBO J.* 15, 810–816.

Vagin, A., Teplyakov, A., 2000. An approach to multi-copy search in molecular replacement. *Acta Crystallogr. D Biol. Crystallogr.* 56 (Pt. 12), 1622–1624.

Vetter, I.R., Wittinghofer, A., 2001. The guanine nucleotide-binding switch in three dimensions. *Science* 294, 1299–1304.

White, M.A., Vale, T., Camonis, J.H., Schaefer, E., Wigler, M.H., 1996. A role for the Ral guanine nucleotide dissociation stimulator in mediating Ras-induced transformation. *J. Biol. Chem.* 271, 16439–16442.

Wolthuis, R.M., de Ruiter, N.D., Cool, R.H., Bos, J.L., 1997. Stimulation of gene induction and cell growth by the Ras effector Rlf. *EMBO J.* 16, 6748–6761.

Yan, C., Liu, D., Li, L., Wempe, M.F., Guin, S., Khanna, M., Meier, J., Hoffman, B., Owens, C., Wysoczynski, C.L., et al., 2014. Discovery and characterization of small molecules that target the GTPase Ral. *Nature* 515, 443–447.